



Scholars Research Library

Der Pharmacia Lettre, 2016, 8 (17):95-105
(<http://scholarsresearchlibrary.com/archive.html>)



Design of Prolonged Release Nanoparticulate Formulation for Diltiazem Hydrochloride by Central Composite Design

Sarmistha Saha^{1,2} and Ravada Ramesh¹

¹Dr. H. L. Thimmegowda College of Pharmacy, Kengal, Channapatna, Ramanagaram, 562161, Karnataka, India

²Research Scholar, Pacific University, Airport Road, Pratap Nagar Extension, Debari, Udaipur, 313024, Rajasthan, India

ABSTRACT

An attempt was made to prepare and optimize prolonged release nanoparticulate formulation for diltiazem hydrochloride using bioadhesive polymer gelatin by desolvation method, to deliver drug at a controlled rate to its absorption window and thereby improve bioavailability. On the basis of screening studies amount of gelatin and glutaraldehyde were selected for the optimization study, using face centered central composite design (CCD), with $\alpha=1$. The optimized formulation was evaluated for morphology, stability and X-ray imaging for in-vivo evaluation of the mucoadhesive property. The optimized nanoparticles were found to be discrete and spherical in shape. Accelerated stability studies as per ICH guidelines revealed that there were no significant changes after 6 months. The X-ray studies revealed even after 10 h, NPs were observed to be adhered in the gastric region, since the mucoadhesive property of NPs delay influx at the pylorus. But the barium sulphate suspension (control) was cleared off completely from the stomach within 4 h. The results suggest that the bioavailability of Diltiazem HCl may be enhanced due to the extended retention of mucoadhesive nanoparticles in upper GIT.

Keywords: Optimization, mucoadhesion, nanoparticles, gelatin, pharmacokinetics.

INTRODUCTION

The oral route of drug administration is the most convenient and commonly used method of drug delivery due to their considerable therapeutic advantages such as ease of administration, patient compliance and flexibility in formulation. However, this route has several physiological problems, such as inability to restrain and locate the controlled drug delivery system within the desired region of the gastrointestinal tract (GIT) due to variable gastric emptying and motility[1,2]. These difficulties have prompted researchers to design a drug delivery system which can stay in the stomach for prolonged and predictable period[3,4]. Different methodologies have been reported in the literature to increase the gastric retention of drugs, like intra-gastric floating systems, hydro dynamically balanced systems, extendable or expandable, microporous compartment system, microballons, Bio/Muco-adhesive systems, high-density systems and super porous biodegradable hydro gel systems⁵.

Diltiazem HCl (DTZ) is an antihypertensive agent that antagonizes the action of beta-1 receptor. DTZ when given orally is well absorbed from the gastrointestinal tract and is subject to an extensive first-pass effect. DTZ undergoes extensive metabolism in which only 2% to 4% of the unchanged drug appears in the urine. Drugs which induce or inhibit hepatic microsomal enzymes may alter DTZ disposition⁶. It has been reported that the absolute bioavailability of DTZ when given orally is 30-40%. The biological half-life of DTZ is 4-6 hour and the main site of absorption is proximal small intestine⁷. The reduced bioavailability of DTZ may be because of transportation of dosage form from the region of absorption window to site where it is less absorbed. Therefore there was a need to increase gastroretention time of dosage form so that drug would be available at the site of absorption and results in

improved bioavailability. Hence drug like diltiazem is considered as a suitable candidate for the design of nanoparticulate drug delivery system with a view to improve oral bioavailability and patient compliance

When mucoadhesive nanoparticles (NPs) are taken by oral route, the NPs will network with the GI surface and build up adhesive bonds with diverse elements of the mucosa. This adhesive event may result in either: (a) an enhancement of the retention time of formulation in contact with mucosa, (b) a confinement of formulation in a specified area of gut. Upon adhesion to the gut mucosa, these NPs would enhance transfer of drug to the blood by a several mechanism involving shielding of the drug within NPs against deprivation and establishes a drug concentration gradient favoring the absorption[8-9].

The conventional one variable at a time (OVAT) approach of formulation development has some pitfalls, like being exhaustive, expensive, and incompetent to disclose interactions. Additionally, the OVAT approach results only in “just satisfactory” solutions and one cannot establish “cause and effect” relationships by OVAT. The systematic optimization approaches reduce inconsistencies, which includes the utilization of appropriate experimental designs along with the creation of mathematical equations and graphical upshots, representing a full portrait of variation of the responses as a function of the factors is known as Design of Experiments (DoE)[10-13]. One of the techniques in DoE which investigate pharmaceutical problems with the least number of experiments and results in selection of the optimal composition for a formulation is Central Composite Design (CCD). The objective of the present work was to optimize mucoadhesive gastroretentive NPs of DTZ by application of DoE. Gelatin was selected as a mucoadhesive polymer to prepare gastroretentive NPs as they strengthen the contact between the site of absorption and dosage form, in this manner reducing the luminal diffusion pathway of the drug and lead to substantial improvements in oral drug delivery.

MATERIALS AND METHODS

Materials

DTZ was a gift sample from M/s Modern Laboratories Pvt. Ltd., Indore, India. Dialysis tubing's (cut-off 12 kDa) were procured from Sigma (USA). Gelatin and Pluronic F-68 were purchased from HiMedia Laboratories Pvt. Ltd., Mumbai, India. All other solvents and ingredients used were of analytical grade.

Experimental Design

Systematic optimization was done by selecting the response, finding the most significant factors and establishing the correlation between responses and factors by response surface methodology (RSM). On the basis of screening studies amount of gelatin and glutaraldehyde were selected for the optimization study, using face centered CCD (with $\alpha=1$), which allows assessment of curvature and makes the design to be rotatable^{14,15}. A two factor, three level designs was used to explore the RSM using Design-Expert software (Trial Version 8.0.6, Stat-Ease Inc., MN). The coded and actual values of the independent variables along with constraints for dependent variables are given in Table 1. As per the CCD matrix four factorial points, four axial points and five replicated center point formulations were prepared¹⁶. The amount of gelatin (X_1) and glutaraldehyde (X_2) used to prepare the formulations and the subsequent results for dependent variables are given in Table 2.

Table 1 Variables in Central Composite Design

Factors	Level used, Actual (coded)		
	Low (-1)	Intermediate (0)	High (+1)
X1 = Amount of Gelatin (mg)	300	500	700
X2 = Amount of Glutaraldehyde (mL)	1.0	1.5	2.0
Dependent Variables	Response Constraints		
Y1 = Particle size (nm)	Minimize (150-500)		
Y2 = Polydispersity index	Minimize (0.20-0.40)		
Y3 = Entrapment efficiency (%)	Maximize (45-60)		
Y4 = Drug loading (%)	Maximize (55-70)		
Y5 = T60 (h)	Maximize (9.0-15.0)		
Y6 = Q6 (%)	Minimize (14-30)		
Y7 = Mucoadhesive strength (g)	Maximize (7.0-12.0)		

Where, T60: time required to release 60% of drug; Q6: amount of drug released in 6 h.

Table 2 Observed responses in CCD for Diltiazem HCl nanoparticles

Batch	Independent		Dependent Variables						
	X ₁ (mg)	X ₂	PS	PDI	BA (g)	Q6	T60%	EE	DL
CCDF1	-1	-1	608.6	0.450	12.32	38.45	9.40	45.46	58.51
CCDF2	1	-1	220.8	0.302	8.45	16.01	14.50	49.15	61.04
CCDF3	-1	1	508.9	0.367	11.55	26.14	12.45	52.45	62.01
CCDF4	1	1	446.2	0.530	7.21	13.94	15.50	42.02	57.51
CCDF5	-1	0	72-2.9	0.651	12.06	28.05	11.48	60.41	68.41
CCDF6	1	0	286.6	0.500	7.85	15.73	14.97	56.62	60.45
CCDF7	0	-1	151.0	0.398	11.02	30.12	12.40	44.45	53.47
CCDF8	0	1	764.5	0.738	9.01	16.14	13.75	44.17	58.71
CCDF9	0	0	549.1	0.228	10.44	20.35	12.90	47.12	64.48
CCDF10	0	0	563.1	0.493	11.01	22.15	13.00	52.87	58.99
CCDF11	0	0	544.1	0.210	10.04	21.17	12.95	51.91	59.95
CCDF12	0	0	585.2	0.312	9.51	21.48	12.95	50.15	57.47
CCDF13	0	0	524.8	0.718	9.75	21.95	13.03	49.61	58.04

Where, X₁: Amount of gelatin (mg), X₂: Amount of Glutaraldehyde (mL).

Preparation of Nanoparticles

Nanoparticles of DTZ were prepared by desolvation method as described by Coester *et al.* with slight modification. Gelatin was dissolved in distilled water (50 mL) under gentle heating and DTZ (120 mg) was then added to the polymeric solution. Poloxamer 237 was then added as stabilizer and the pH of solution was adjusted (by 1N hydrochloric acid or 1N sodium hydroxide). Then 50 mL of acetone was added at specified addition rate, after 10 min of acetone addition glutaraldehyde was added for cross-linking of nanoparticles. After stirring for specified time the nanoparticles were purified by three fold centrifugation (15000 g for 30 min at 4°C) and redispersion in 10 mL mixture of acetone: water (3:7). The supernatant was removed and the pellets were resuspended in distilled water and finally, the nanoparticles were freeze-dried and stored in vials¹⁷⁻²¹.

Evaluation Parameters

Particle Size and Polydispersity Index

Average particle size (average particle size) and particle size distribution (polydispersity index) were determined using the zeta sizer (Zetasizer- ZEN 2600 Malvern Instrument Ltd., Worcestershire, UK) equipped with the Malvern PCS software. For analysis nanoparticles were diluted five times with 0.45 µm membrane filtered bidistilled water²².

Entrapment Efficiency

For determination of entrapment efficiency, the amount of drug present in the clear supernatant after centrifugation was determined (w) by UV spectrophotometer at 237 nm (UV-1700 Spectrophotometer, Shimadzu Scientific Instruments, Inc. Maryland, USA). The amount of drug in supernatant was then subtracted from the total amount of drug added during the preparation (W)²³. Percentage drug entrapment was obtained by using following equation

$$\% \text{ Drug Entrapment} = (W-w) \times 100 / W$$

Drug Loading

The drug content in the nanoparticles was determined by crushing the drug loaded nanoparticles (10 mg) followed by immersing them in 100 mL simulated gastric fluid (SGF, pH 1.2, without enzymes) with agitating for 12 h at room temperature. The drug concentration was determined spectrophotometrically after filtration through a 0.45 µm membrane filter (Millipore) at the wavelength of 237 nm. The filtered solution from the empty nanoparticles (without drug) was taken as blank. The drug loading (DL) was calculated according to the equation given below, all samples were analyzed in triplicate²⁴:

$$DL (\%) = WD/WT \times 100$$

Where, DL: drug loading; WD: the weight of the drug loaded in the nanoparticles;
WT: the total weight of the nanoparticles.

Drug Release Study

The *in vitro* drug release studies were performed by dialysis membrane diffusion technique using glass tube of 10 cm length open at its both ends having 2.5 cm diameter. The dialysis membrane of 12,000 Mwco (Spectra por, Sigma, USA) was used for release study, because it retains nanoparticles and allows free drug to diffuse in the release media. The lower end of the glass tube was covered with the pretreated membrane to keep the nanoparticulate formulation on the donor side. The nanoparticles (equivalent to 10 mg of drug) were placed in donor

compartment by dispersing in 3 mL of SGF (pH 1.2) where the drug was allowed to freely diffuse over the receptor compartment containing 100 mL of SGF (pH 1.2). The entire system was kept at $37\pm 0.5^\circ\text{C}$ with continuous magnetic stirring at 100 rpm. Samples of 5 mL were withdrawn at predetermined time intervals (0.5, 1, 2, 4, 6, 9, 12, 15, 18 and 24 h) and replaced with fresh SGF^{22,25}. The withdrawn samples were suitably diluted to carry out UV Spectrophotometric analysis at 237 nm. The results of *in-vitro* drug release profiles of all the formulations were fitted to zero-order, first order, Higuchi's model and Korsmeyer-Peppas equation to establish the mechanism of drug release²⁶⁻²⁸.

Measurement of Bioadhesive strength

Mucoadhesive properties of nanoparticles were evaluated by Texture analyzer (M/s TA. XT. Plus, Stable Microsystem, UK) using porcine gastric mucosa. The method is based on the measurement of shear stress required to break the adhesive bond between a mucosal membrane and the formulation. The formulation is sandwiched between two mucosal membranes fixed on flexible supports in the assemblies for a sufficient period of time. After the adhesive bond has formed, the force (weight) required to separate the bond was recorded as mucoadhesive strength. This parameter was used to compare mucoadhesive property of various formulations.

Stomach of pig was washed with fresh water to remove non-digested food from stomach then placed in SGF at 4°C (used within 6 h). The porcine gastric mucosal membrane was then attached both to the stainless steel probe (using dual side adhesive tape) and on the base of texture analyzer. Probe is then fixed to the mobile arm of the texture analyzer. The 20 mg of nanoparticulate formulation was placed on the membrane placed on lower surface moistened with 2 mL of SGF. The mobile arm with attached membrane was lowered at a rate of 0.5 mm s^{-1} until contact with the formulation was made. A contact force of 20 g was maintained for 300 s, after which the probe was withdrawn from the membrane. After the adhesive bond has formed, the force of detachment (g) required to separate the bond was recorded as mucoadhesive strength¹⁸⁻²⁹.

Data Analysis

ANOVA provision accessible in the software was used to ascertain the statistical validation of the polynomial equations generated by Design Expert[®]. The data was considered statistically significant if p-value was less than 0.05. Feasibility followed by grid searches was carried out to ascertain the compositions of the optimized formulations. With the help of software program minimum and maximum boundaries were set for acceptable responses. In the next step region was highlighted wherein all the responses are within acceptable limit. An optimum was located, within this area, by trading off different responses. Validation of derived polynomial equations and selection of optimized formulation was carried out by preparation of five optimum checkpoint formulations. The percentage prediction error was calculated by comparing experimental values of the responses with the predicted values³⁰⁻³¹.

Morphology

Morphology of optimized formulation VAF3 was carried out by transmission electron microscopy (Hitachi, H-7500 Tokyo, Japan). The aqueous dispersion (one drop) was placed over a 400-mesh carbon coated copper grid followed by negative staining (which provides high contrast in the electron microscope) with phosphotungstic acid solution (3% w/v, adjusted to pH 4.7 with potassium hydroxide). After drying, the sample was viewed in the electron microscope where the NPs appear bright against the darker background of the stain. Digital Micrograph and Soft Imaging Viewer software were used to perform the image capture and analysis, including particle sizing. Scanning electron microscopy (SEM) of the optimized formulation was observed by JSM-6100 (Jeol Ltd. Tokyo, Japan) equipped with a digital camera at 25kV accelerating voltage³².

Stability Studies

Accelerated stability studies of the optimized formulation VAF3 was carried out as per ICH guidelines at $30\pm 2^\circ\text{C}/65\pm 5\%\text{ RH}$ and $40\pm 2^\circ\text{C}/75\pm 5\%\text{ RH}$. The samples were packed in aluminum foil packets. Samples were withdrawn at 0, 3 and 6 months in triplicates and were assessed for particle size, PDI, drug content, T_{60} and Q_6 (ICH, 2003³³).

In-vivo Mucoadhesion Studies

The *in-vivo* evaluation of the bioadhesive property of the optimized formulation was performed by X-ray radio opaque studies using healthy male *Wistar* rats weighing 220-300 g. The rats were separated into two groups each having three animals. Before administration of dosage form animals were fasted for the night with access to water. NPs containing barium sulphate were prepared by desolvation method as applied for the optimized formulation by replacing drug with barium sulphate. The quantity of incorporated barium sulphate was detectable in X-ray photographs. First group of rats was ingested with 2 mL of plain barium sulphate suspension and second group was ingested with nanoparticulate formulation containing barium sulphate with 2 mL of water by using oral feeding

needle. The GI transit behavior of the formulations were observed by taking X-ray photographs at suitable time intervals using fluoroscopy (low energy X-rays, Siemens Fluorovision, Germany). The rats were anaesthetized by chloroform and placed on a kappa board, at 20 cm above the film. The X-ray camera (model DM100p, Domgmun, Korea) was placed 1 m above the film cassette and exposed for 0.05 s at 40 kVp. Film development was carried out by using Direct Digitizer Regius Model 110 (Konica Minolta Medical & Graphic, Inc., Tokyo, Japan) with Image Pilot software (Konica Minolta Medical Imaging Inc, New Jersey, USA). This technique provides a non-invasive method for tracking the nanoparticulate formulation within the GIT³⁴³⁷.

RESULTS

Model Generation

For fitted model the experimental response might be represented by the following regression equation:

$$Y = B_0 + B_1X_1 + B_2X_2 + B_3X_1X_2 + B_4X_1^2 + B_5X_2^2 + B_6X_1^2X_2 + B_7X_1X_2^2 \quad (1)$$

Where, Y is the measured response associated with each factor level combination; B₀ is an intercept; B₁ to B₇ are regression coefficients computed from the observed experimental values of Y from experimental runs; and X₁ and X₂ are the coded levels of independent variables; X₁X₂ and X_i² (i = 1 or 2) represent the interaction and polynomial terms, respectively¹⁶.

Response Surface Analysis

Three dimensional response surface plots for the graphical optimization of DTZ loaded mucoadhesive nanoparticulate system are shown in Fig. 1, which facilitate understanding of the contribution of the variables and their interactions on the responses.

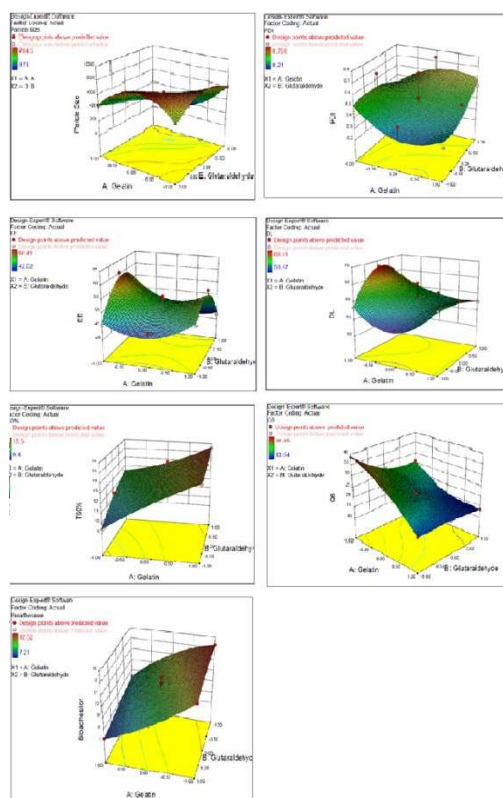


Fig.1. Response Surface Plots Showing the Influence of Gelatin and Glutaraldehyde on response variables.

Validation of Optimization Analysis

For all of the five checkpoint formulations, the results of the evaluation for particle size, PDI, EE, DL, T₆₀, Q₆ and BA were found to be within limits as shown in Table 3. The validity of generated regression equations was evaluated by determination of percentage prediction error.

Table 3 Composition of check-point formulations, experimental results with predicted responses

Form. Code	Composition Gelatin (mg)/ Glutaraldehyde (mL)		Response	Predicted value	Experimental value	Percent error (bias)
	Coded	Actual				
VAF1	0.64/-0.20	628.0/1.4	Particle size	346.4	354.1	2.223
			PDI	0.39	0.47	20.513
			Q6	18.3	18.18	-0.656
			T60%	14.1	14.6	3.546
			% Entrapment efficiency	52.3	55.1	5.354
			% Drug loading	58.9	60.1	2.037
VAF2	0.76/-0.32	652.0/1.34	Bioadhesion study	8.90	9.10	2.247
			Particle size	297.9	272.0	-8.694
			PDI	0.39	0.361	-7.436
			Q6	17.6	17.54	-0.341
			T60%	14.3	14.5	1.399
			% Entrapment efficiency	52.9	51.4	-2.836
VAF3	0.92/-0.60	684/1.2	% Drug loading	59.2	56.9	-3.885
			Bioadhesion study	8.70	8.85	1.724
			Particle size	239.4	240.5	0.459
			PDI	0.43	0.393	-8.605
			Q6	15.8	15.96	1.013
			T60%	14.5	15.0	3.448
VAF4	0.10/-0.38	520/1.31	% Entrapment efficiency	53.1	56.4	6.215
			% Drug loading	60.2	58.7	-2.492
			Bioadhesion study	8.46	8.34	-1.418
			Particle size	399.9	384.3	-3.901
			PDI	0.368	0.389	5.707
			Q6	23.55	23.65	0.425
VAF5	0.09/-0.50	518/1.25	T60%	12.95	12.8	-1.158
			% Entrapment efficiency	49.9	52.4	5.010
			% Drug loading	58.12	62.15	6.934
			Bioadhesion study	10.3	9.9	-3.883
			Particle size	354.6	366.5	3.356
			PDI	0.35	0.38	8.571
VAF5	0.09/-0.50	518/1.25	Q6	24.58	24.91	1.343
			T60%	12.86	12.68	-1.400
			% Entrapment efficiency	55.41	57.45	3.682
			% Drug loading	57.41	60.15	4.773
			Bioadhesion study	10.42	10.9	4.607
Total % Error						2.91
Mean						0.194
Std. Deviation						4.646
±SEM						1.200

***In-vitro* Release Studies**

Comparison of drug release profile of different formulations was carried out by determination of T_{60} (time for 60% of the drug to be released) and Q_6 (cumulative percent drug release in 6 h) values. The release profiles of DTZ from check point formulations are shown in Fig. 2. The mechanism of drug release was determined by linear regression analysis of *in-vitro* dissolution data subjected to zero order, first order kinetic equation, Higuchi's and Korsmeyer-Peppas model.

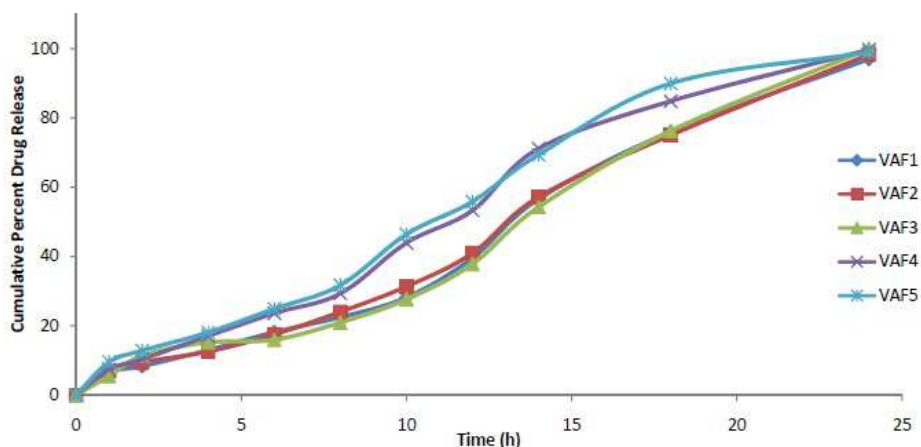


Fig.2. *In-vitro* release profiles of the check point formulations

Optimization

The formulation VAF3 was chosen as optimized formulation depending upon the condition of attaining the minimum PS and percent error.

Morphology of Nanoparticles

Morphology of the optimized formulation VAF3 was observed by TEM (H-7500; Hitachi Ltd., Tokyo, Japan) at 30,000x magnification as shown in Fig. 3. The surface and inner part of the optimized formulation VAF3 were observed via scanning electron microscopy JSM-6100 (Jeol Ltd. Tokyo, Japan) equipped with a digital camera at 25kV accelerating voltage as shown in Fig. 4.

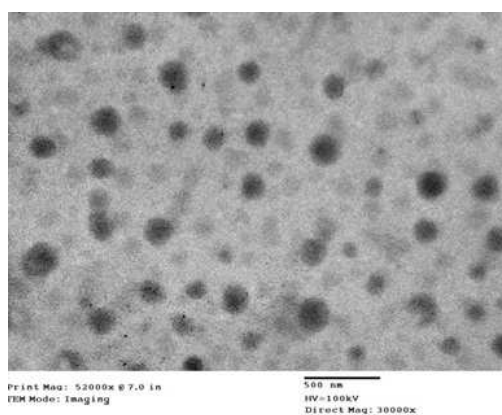


Fig.3. TEM (30000x) of optimized formulation (VAF3)

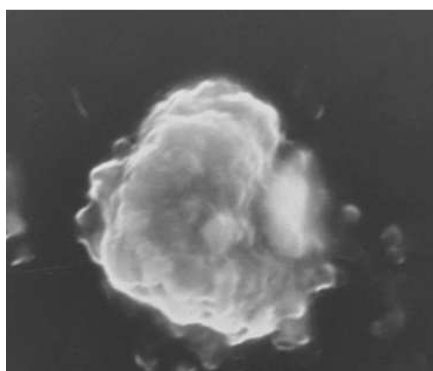


Fig.4. SEM (30000x) of optimized formulation (VAF3)

Stability Studies

Accelerated stability studies of the optimized formulation VAF3 were carried out as per ICH guidelines at $30^{\circ} \pm 2^{\circ}\text{C}/65 \pm 5\% \text{RH}$ and $40^{\circ} \pm 2^{\circ}\text{C}/75 \pm 5\% \text{RH}$ for 6 months. The samples were tested for PS, PDI, assay, T_{60} and Q_6 at

0, 3 and 6 months. Statistical analysis was performed on the data obtained by using 't' test and data are shown in Table 4.

Table 4 Stability studies of optimized formulation VAF3

Storage	Storage Period (Months)	PS (nm)	PDI	Assay (%)	T ₆₀ (%)	Q ₆ (h)
30° ± 2°C & 65 ± 5% RH	0	240.5±10.4	0.393±0.04	100.00±1.86	15.00±0.53	15.96±0.48
	3	238.3±15.4	0.425 ±0.06	98.31±2.10	15.65±0.85	14.65±0.84
	6	245.5±11.4	0.431±0.10	97.11±1.90	16.01±0.79	14.18±1.64
	t value (ns)	0.561	0.611	1.883	1.839	1.804
40° ± 2°C & 75 ± 5% RH	0	240.5 ±10.4	0.393±0.04	100.00±1.86	15.00±0.53	15.96±0.35
	3	246.4 ±12.4	0.434±0.09	97.49±2.15	16.00±0.48	14.01±2.45
	6	248.5 ±9.45	0.447±0.11	95.98±2.54	16.23±1.45	13.89±2.15
	t value (ns)	0.986	0.799	2.212	1.380	1.628

Data expressed as mean ±SD (n = 3); ns = statistically not significant (p<0.05), table value of 't' (two tailed) was 2.776 (DF = 4).

***In-vivo* Mucoadhesion Studies**

The results for *in-vivo* mucoadhesion studies on *Wistar* rats after oral administration of barium sulphate suspension (control) and bioadhesive NPs are shown in Fig. 5 (a) and (b) respectively. X-ray images of rats were taken prior to the administration of the NPs to verify that the observed opaque substance in the stomach of rats was not due to some foreign matter already existed in the stomach.

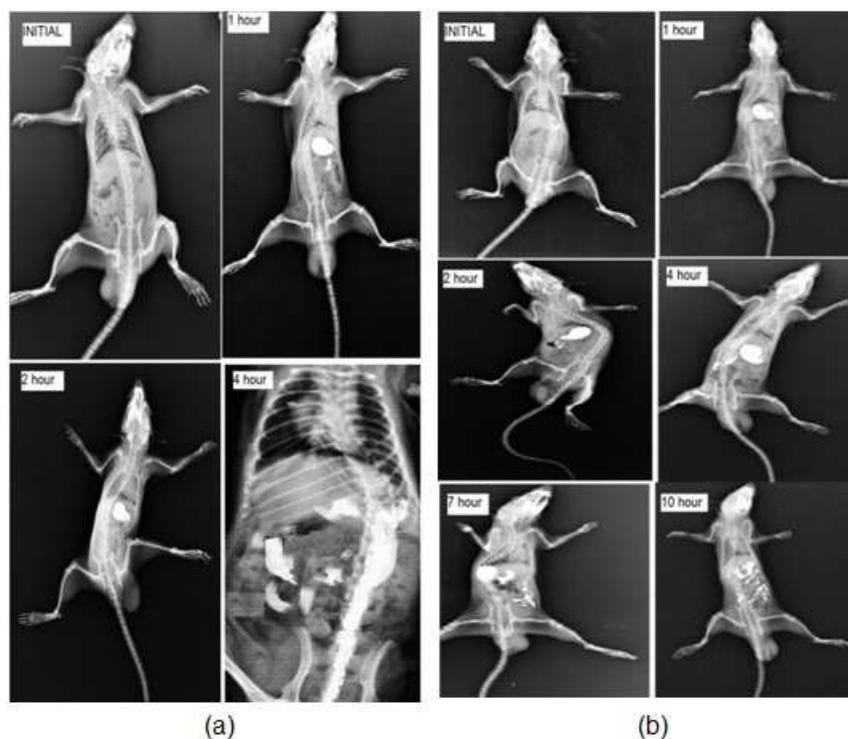


Fig.5. X-ray images for (a) Barium sulphate suspension (Control) (b) Bioadhesive nanoparticles after oral administration to rats

DISCUSSION

From response surface methodology it was observed that particle size increases maximum at intermediate level and decreases at higher level of polymer and glutaraldehyde. The value of particle size decreases with increase in concentration of gelatin at all levels of glutaraldehyde (maximum effect at lower level), which may be due to formation of small droplets of polymeric system before final cross linking. With increase in the concentration of gelatin the value of PDI decreases, while increases with increase in the level of glutaraldehyde. At lower level of glutaraldehyde PDI decreases with increase in polymer concentration while at intermediate and higher level of glutaraldehyde the change in PDI is minimal with increase in polymer concentration.

The entrapment efficiency first decreases and then increases as the polymer concentration is increases at low level of glutaraldehyde, at intermediate level of glutaraldehyde there is slight decrease initially with increase in gelatin concentration. The value of entrapment efficiency first increases and then decreases as glutaraldehyde concentration is increased. The drug loading first decreases and then increases as the polymer concentration is increases at low level of glutaraldehyde, at intermediate level of glutaraldehyde there is slight decrease initially with increase in

gelatin concentration and at higher level the effect was minimal. The value of drug loading first increases and then decreases as glutaraldehyde concentration is increased at lower level, increased at intermediate level and minimal effect at higher level of gelatin.

The $T_{60\%}$ increases as the polymer concentration is increased at all levels of glutaraldehyde. The value of $T_{60\%}$ also increases as glutaraldehyde concentration is increased at lower, minimal effect at intermediate and higher level of gelatin. This may be attributed to release retarding property of gelatin and cross-linking effect of glutaraldehyde. The Q_6 decreases as the polymer concentration is increased at all levels of glutaraldehyde. The value of Q_6 also increases as glutaraldehyde concentration is increased at lower and intermediate level with very less effect at higher level of gelatin. This also may be attributed to release retarding property of gelatin and cross-linking effect of glutaraldehyde. The bioadhesion decreases as the polymer concentration is increased at all levels of glutaraldehyde. The value of bioadhesion also decreases as glutaraldehyde concentration is increased at all level of gelatin which may be due to cross-linking effect of glutaraldehyde.

From the data of Table 3 it was observed that absolute percentage bias for the response variables was in the range of -8.69% to 8.57 (Except error of PDI for VAF i.e. 20.51%), whereas the extent of overall percent prediction error was less, i.e., 0.194 ± 1.20 . The low magnitudes of errors demonstrated the high prognostic capability of optimization technique (CCD).

It was observed from the *in-vitro* drug release data that validation formulations displayed zero order drug release kinetics as zero order plots were found to be fairly linear as indicated by their high regression values (R^2 values in the range of 0.959 to 0.981) than first order plots. Drug release data fitted well (R^2 values in the range of 0.852 to 0.937) to Higuchi's equation indicating drug release by diffusion mechanism. The Korsmeyer-Peppas equation slope (n) values were in the range of 0.797 to 0.882 ($0.45 < n < 0.89$) indicated drug release by non-Fickian transport (anomalous transport). These data reveal that releases of DTZ from prepared formulations were found to follow zero order release kinetics with non-Fickian diffusion mechanism³⁸⁻³⁹.

The optimized formulation VAF3 was having PS of 240.5 nm, PDI of 0.393, EE of 56.4%, DL of 58.7%; T_{60} was 15.0 h, Q_6 was 15.96% and BA was 8.34 g.

The TEM characterization revealed that the nanoparticles are discrete and spherical in shape. However, some variation in size distribution was observed in the TEM, which might be attributed to an uncontrolled cross-linking occurring during the formation of nanoparticles. SEM showed some fragments on the surface of nanoparticles with no agglomeration or aggregation.

From the data of table 4 it was observed that optimized formulation VAF3 shown minor aggregation of nanoparticles arisen which resulted in insignificant rise in average size of NPs and thereby change in PDI. For all the parameters 't' values calculated after six months of storage at both storage conditions were less against the table value of 2.776 ($p < 0.05$). These results indicate that during storage at $30^\circ \pm 2^\circ\text{C}/65 \pm 5\% \text{RH}$ and $40^\circ \pm 2^\circ\text{C}/75 \pm 5\% \text{RH}$ for 6 months there were no significant changes in PS, PDI, assay and dissolution profile of the optimized formulation VAF3.

It was observed that the barium sulphate suspension (control) was cleared off completely from the stomach within 4 h as observed in Fig. 5 (a). But most of the bioadhesive NPs were in the stomach for about 2-4 h, followed by passage of some NPs into the upper intestinal tract where they stayed for about 2 h, followed by jejunum and ileum up to 2-4 h and subsequently in colon during the period of study as shown in Fig. 5 (b). After 10 h of administration, NPs were observed to be adhered in the gastric region, since the bioadhesive nature of NPs delay entry at the lower part of GIT.

CONCLUSION

In the present study, gastroretentive mucoadhesive NPs of DTZ were prepared by desolvation method and successfully optimized by CCD. The statistical models generated for the experimental design were found to be valid for predicting the values of the response parameters at selected values of the formulation factors within the design space. *In-vitro* drug release studies demonstrated that optimized formulation resulted in sustained release of drug over a period of 24 h, by non-Fickian diffusion mechanism with zero order release kinetics, indicating drug release by both polymer relaxation and diffusion of drug from hydrated matrix. The optimized NPs were discrete spherical NPs and accelerated stability studies (as per ICH guidelines) concluded that the optimized formulation VAF3 was stable during 6 months of study period. From the results of X-ray studies, it was concluded that the optimized formulation was retained in the stomach and upper part of small intestine for an extended time and thus aid in absorption of drug at its absorption site. The optimized formulation may give considerable biomedical benefits over

conventional tablet formulation. Hence, prolonged release nanoparticulate formulation for DTZ signifies a practical approach for targeting release of drug at its absorption window, sustaining release of drug and increasing bioavailability.

REFERENCES

- [1] Bechgaard H and Ladefoged K. *Journal of Pharmacy and Pharmacology*. 30(11); **1978**: 690-692.
- [2] Kharia AA, Singhai AK and Verma R. *International Journal of Pharmaceutical Sciences and Nanotechnology*. 4(4); **2012**: 1557-1562.
- [3] Deshpande AA, Rhodes TN and Shah H. *Drug Development and Industrial Pharmacy*. 22; **1996**: 531-539.
- [4] Hwang SJ, Park H and Park K. *Critical Reviews in Therapeutic Drug Carrier Systems*. 15; **1998**: 243-248.
- [5] Singh BN and Kim KH. *Journal of Controlled Release* 63; **2000**: 235-239.
- [6] Lee Y, Lee M and Shim C. *International Journal of Pharmaceutics*. 76; **1991**: 71-76.
- [7] Brunton L, Lazo J and Parker K. Goodman and Gillman's Pharmacological Basis of therapeutics, McGraw-Hill, Medical Publishing Division, New Delhi. **2008**:11; pp.1818-1820.
- [8] Ponchel G and Irache J. *Advanced Drug Delivery Reviews*., 34(2-3); **1998**: 191-219.
- [9] Irache JM, Huici M, Konecny M, Espuelas S, Campanero MA and Arbos P. *Molecules*. 10(1); **2005**: 126-145.
- [10] Schwartz JB, O'Connor RE and Schnaare RL. Optimization techniques in pharmaceutical formulation and processing, in: Banker, G.S. and Rhodes, C.T. (Eds.), Modern Pharmaceutics. Informa Healthcare, New York, **2009**: pp. 607-626.
- [11] Singh B, Chakkal SK and Ahuja N. *AAPS PharmSciTech* (. 7(1); **2006**: E1-E10.
- [12] Singh B, Kumar R and Ahuja N. *Critical Reviews in Therapeutic Drug Carrier Systems*. 22(1); **2005**: 27-105.
- [13] Singh B, Pahuja S, Kapil R and Ahuja N. *Acta Pharmaceutica*. 59(1); **2009**: 1-13.
- [14] Saha S and Ramesh R. *American Journal of PharmTech Research*. 6(2); **2016**: 481-492.
- [15] Xu X, Khan MA and Burgess DJ. *International Journal of Pharmaceutics*. 423(2); **2012**: 543-553.
- [16] Hao J, Wang F, Wang X, Zhang D, Bi Y, Gao Y, Zhao X and Zhang Q. *European Federation for Pharmaceutical Sciences*. 47(2); **2012**: 497-505.
- [17] Coester CJ, Langer K, van Briesen H and Kreuter J. *Journal of Microencapsulation*. 17(2); **2000**: 187-193.
- [18] Kharia AA and Singhai AK. *ISRN Nanomaterials*, Vol. **2013**; **2013**: 1-8.
- [19] Marty JJ, Oppenheim RC and Speiser P. *Pharmaceutica Acta Helvetica*. 53(1); **1978**: 17-23.
- [20] Ofokansi K, Winter G, Fricker G and Coester C. *European Journal of Pharmaceutics and Biopharmaceutics*. 76(1); **2010**: 1-9.
- [21] Saraogi GK, Gupta P, Gupta UD, Jain NK and Agrawal GP. *International Journal of Pharmaceutics*. 385(1-2); **2010**: 143-149.
- [22] Elshafeey AH, Kamel AO and Awad GA. *Colloids and Surfaces B: Biointerfaces* 75(2); **2010**: 398-404.
- [23] Das S, Banerjee R and Bellare J. *Trends in Biomaterials and Artificial Organs*. 18(2); **2005**: 203-211.
- [24] Ma N, Xu L, Wang Q, Zhang X, Zhang W, Li Y, Jin L and Li S. *International Journal of Pharmaceutics*. 358(1-2); **2008**: 82-90.
- [25] Kamel AO, Awad GA, Geneidi AS and Mortada ND. *AAPS PharmSciTech*. 10(4); **2009**: 1427-1436.
- [26] Costa P and Sousa Lobo JM. *European Journal of Pharmaceutical Sciences*. 13(2); **2001**: 123-133.
- [27] Dash S, Murthy PN, Nath L and Chowdhury P. *Acta Poloniae Pharmaceutica*. 67(3); **2010**: 217-223.
- [28] Yuce M. and Canefe K. *Turkish Journal of Pharmaceutical Sciences*. 5(3); **2008**: 129-142.
- [29] Thirawong N, Nunthanid J, Puttipipatkachorn S and Sriamornsak P. *European Journal of Pharmaceutics and Biopharmaceutics*. 67(1); **2007**: 132-140.
- [30] Xu X, Khan MA and Burgess DJ. *International Journal of Pharmaceutics*. 423(2); **2012**: 543-553.
- [31] Motwani SK, Chopra S, Talegaonkar S, Kohli K, Ahmad FJ and Khar RK. *European Journal of Pharmaceutics and Biopharmaceutics*. 68(3); **2008**: 513-525.
- [32] Nahar M, Mishra D, Dubey V and Jain NK. *Nanomedicine: Nanotechnology, Biology and Medicine*. Vol. 4(3); **2008**: 252-261.
- [33] ICH, International conference on harmonisation of technical requirements for registration of pharmaceuticals for human use. Stability testing of new drug substances and products, Q1A (R2), Geneva, Switzerland, February **2003**.
- [34] Saphier S, Rosner A, Brandeis R and Karton Y. *International Journal of Pharmaceutics*., Vol. 388(1-2); **2010**: 190-195.
- [35] Ashwini RM, Mangesh RB, Rahul RP, Nilkanth SP and Devaki CU. *American Journal of the Medical Sciences*. Vol. 2(4); **2012**: 62-70.
- [36] Ramteke S, Maheshwari RB and Jain NK. *Ind. J. Pharm. Sci.*, Vol. 68(4); **2008**: 479-484.
- [37] Alli SMA, Ali SMA, Fatmah K and Fatmah NY. *International Journal of Life Science and Pharma Research*. Vol. 1(1); **2011**: 41-59.
- [38] Althaf AS, Seshadri T, Sivakranth M and Khair US. *Der Pharmacia Sinica*. Vol. 1(2); **2010**: 61-76.

[39] Sahoo S, Chakraborti CK and Behera PK. *Journal of Chemical and Pharmaceutical Research*. Vol. 4(4); 2012: 2268-2284.